Near-ideal strength in metal nanotubes revealed by atomistic simulations

Mingfei Sun, Fei Xiao, and Chuang Deng

Citation: Appl. Phys. Lett. **103**, 231911 (2013); doi: 10.1063/1.4841995
View online: http://dx.doi.org/10.1063/1.4841995
View Table of Contents: http://apl.aip.org/resource/1/APPLAB/v103/i23
Published by the AIP Publishing LLC.

Near-ideal strength in metal nanotubes revealed by atomistic simulations

Mingfei Sun,[1] Fei Xiao,[1] and Chuang Deng[2,a)]
[1]Department of Materials Science, Fudan University, 220 Handan Road, Shanghai 200433, China
[2]Department of Mechanical and Manufacturing Engineering, The University of Manitoba, 15Gillson Street, Winnipeg, Manitoba R3T 5V6, Canada

(Received 12 October 2013; accepted 21 November 2013; published online 6 December 2013)

Here we report extraordinary mechanical properties revealed by atomistic simulations in metal nanotubes with hollow interior that have been long overlooked. Particularly, the yield strength in [1 1 1] Au nanotubes is found to be up to 60% higher than the corresponding solid Au nanowire, which approaches the theoretical ideal strength in Au. Furthermore, a remarkable transition from sharp to smooth yielding is observed in Au nanotubes with decreasing wall thickness. The ultrahigh tensile strength in [1 1 1] Au nanotube might originate from the repulsive image force exerted by the interior surface against dislocation nucleation from the outer surface. [http://dx.doi.org/10.1063/1.4841995]

Metal nanowires (NWs) have been known for their ultrahigh strength and elasticity for a while, and size effect of "smaller is stronger" has been regarded as a signature of metal NWs.[1–7] Besides the nanosized diameter, other characteristic sizes may also arise in metal NWs from various microstructural defects such as stacking faults and grain boundaries.[2,4,5,8] Both experimental investigations[2,4,5] and atomistic simulations[2,9,10] have revealed that the characteristic sizes of internal microstructural defects played an important role on the mechanical properties of metal NWs. The synergistic size effects between external and internal structural features have inspired the design of various novel one-dimensional nanostructures to achieve unique mechanical properties via the introduction of special structural defects.[2,9] In particular, near-ideal strength in [1 1 1]-oriented Au NWs containing angstrom scale twins and special surface facets was reported from both atomistic simulations[9] and *in situ* tensile experiments.[2,11]

In recent years, an alternative approach of manipulating the structure and mechanical properties of metal NWs by "subtraction" instead of "addition" has drawn considerable attention as stimulated by the extraordinary mechanical properties of carbon nanotubes (CNTs).[12,13] A category of special metal NWs of hollow interior, or metal nanotubes (NTs), have thus emerged. Nowadays, various techniques[14–16] have been developed to synthesize NTs in different metals such as Au,[17–20] Ag,[21,22] and Cu.[23] It is likely that the hollow interior of metal NTs may significantly influence their mechanical properties by forming a second interface (the interior surface as opposed to the exterior surface) and one additional feature size (the wall thickness as opposed to the sample diameter) as compared to the corresponding solid metal NWs.

Nevertheless, metal NTs have been long overlooked, and to date no experimental work has been reported on the mechanical characterization of metal NTs; only very few investigations through molecular dynamics (MD) simulations have been performed. Specifically, Ji and Park[24] investigated the elasticity of squared Cu NTs oriented along [1 0 0] and [1 1 0] under tensile deformation by MD. They found that the tensile yield strength, yield strain, and Young's modulus in Cu NTs strongly depended on the wall thickness in addition to the NT orientation and the outer diameter. However, only limited strengthening or even weakening was observed in [1 1 0] and [1 0 0] Cu NTs in comparison with the corresponding solid Cu NWs.[24] Furthermore, Ji and Park[24] only studied NTs when the wall was thick enough so that the NTs remained single crystalline and were free of structural defects. Nevertheless, the wall thickness of experimentally synthesized metal NTs could vary from a few atom layers[20,22] to tens of nanometers.[14,19] Past MD simulations have shown that the surface stress in metal NWs significantly increased as the NW diameter decreased; for example, surface stresses alone can cause [1 0 0] Au NWs to transform from a face-centred-cubic (fcc) structure to a body-centred-tetragonal structure when the NW cross-sectional area was below 4 nm.[25] It is thus expected that when the wall thickness of metal NTs was reduced to as thin as a few atom layers, dramatic structural transformation may occur because essentially all atoms in the NT became surface; the existence of one-atom-layer thick metal NTs has been confirmed by experimental observations[20,22] and first principle computations.[26] Therefore, it is interesting to investigate how the surface stress would influence the morphology and mechanical properties of metal NTs when the NT wall is severely thinned.

The aim of this work is to characterize the size- and orientation-dependent strength and elasticity in Au NTs under uniaxial tensile deformation by using MD simulations. In particular, Au NTs of extremely thin wall will be investigated so that the surface stress induced structural change and its influence on the mechanical properties of metal NTs can be evaluated.

The simulations were performed using LAMMPS[27] with a timestep of 5 fs. The interatomic forces were characterized by embedded-atom-method potentials for Au.[28] Cylindrical NTs oriented along [1 0 0], [1 1 0], and [1 1 1] directions, respectively, were created with fixed length of ~52 nm. As shown in Figure 1, the radius of outer surface, radius of inner surface, and the wall thickness of a NT were defined as R, r, and t, respectively. A periodic boundary condition was

a)Author to whom correspondence should be addressed. Electronic mail: dengc@ad.umanitoba.ca. Tel.: +1 204 272 2662.

imposed along the NT axis (z direction) while the NT was kept free in the other directions. Tensile deformation was performed at 300 K and a constant strain rate of $10^8\,s^{-1}$ along the axis using the canonical ensemble (NVT, constant volume and constant temperature). The tensile stress was calculated by adding the local Virial atomic stress[29] along the loading direction over all atoms and dividing by the deformed NT volume. AtomEye[30] was used to visualize the atomistic configurations.

Each model was relaxed for 100 ps under zero stress and at 300 K prior to the tensile deformation. It was found that the morphologies of metal NTs would be significantly affected when the wall thickness was small as compared to the outer diameter, which can be characterized by the ratio of the wall thickness to the outer radius, t/R. Some representative atomistic configurations were shown in Figure 1(a) for relaxed Au NTs with fixed wall thickness ($t = 2$ nm) but varying outer radius R. It was found that with decreasing t/R (increasing R while fixing t), the relaxed NT transformed from perfect single crystalline structure to that with structural defects such as dislocations and stacking faults as highlighted by the dashed circles in Figure 1(a). Similar trend has been observed while fixing R but decreasing t. When t/R was further reduced, the plastic deformation induced by the surface stress was so strong that the surface morphology would be severely changed, e.g., Au NTs with outer radius $R = 8$ nm and $t = 2$ nm in Figure 1(a) and Au NTs with outer radius $R = 5$ nm and wall thickness $t = 0.5$ nm in Figure 1(b). The influence of such structural changes on the yield strength and elasticity of metal NTs was shown below.

Figures 2(a)–2(c) showed the tensile stress-strain curves of Au NTs of fixed outer radius $R = 5$ nm but varying wall thickness from $t = 0.5$ nm to 4 nm oriented along [1 0 0], [1 1 0], and [1 1 1], respectively. The corresponding solid NWs were also simulated for comparison. It is interesting to note from the stress-strain curves that regardless the axial orientation, the solid NWs all showed sharp yielding phenomenon with no strain hardening (e.g., the stress dropped significantly beyond the yield point). The metal NTs, on the other hand, showed a remarkable transition from sharp yielding with no strain hardening to a relatively smooth yielding with pronounced strain hardening as the NT wall thickness was reduced to 1 nm and below. The insets of Figure 2 confirmed that when the NT wall thickness t was 2 nm and above, the Au NTs (including NW) were crystalline, and the yielding in them was dominated by surface nucleation of $\{1\,1\,1\}\langle 1\,1\,2\rangle$ Shockley partial dislocations. On the contrary, when t was reduced to 1 nm and below, a large number of defects, such as stacking faults and dislocations, can be formed due to the strong surface stress even before any external loading was applied (Figure 1(b)). The pre-formed structural defects can serve as both dislocation nucleation sources and obstacles to dislocation migration. As a result, the yielding and plasticity in Au NTs with the wall thickness $t \leq 1$ nm were found to be similar to that in polycrystalline

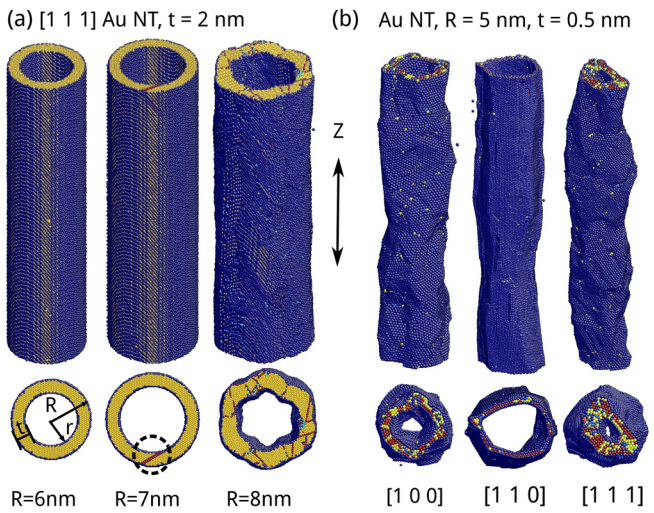

FIG. 1. Side and top view of the atomistic configurations of relaxed Au NTs (a) oriented along [1 1 1] direction with wall thickness $t = 2$ nm and outer radius $R = 6$ nm, 7 nm, and 8 nm and (b) oriented along [1 0 0], [1 1 0], and [1 1 1] directions with wall thickness $t = 0.5$ nm and outer radius $R = 5$ nm. The dashed circles highlight the dislocations and stacking faults formed during the relaxation. The atom colors correspond to the local lattice orientation.

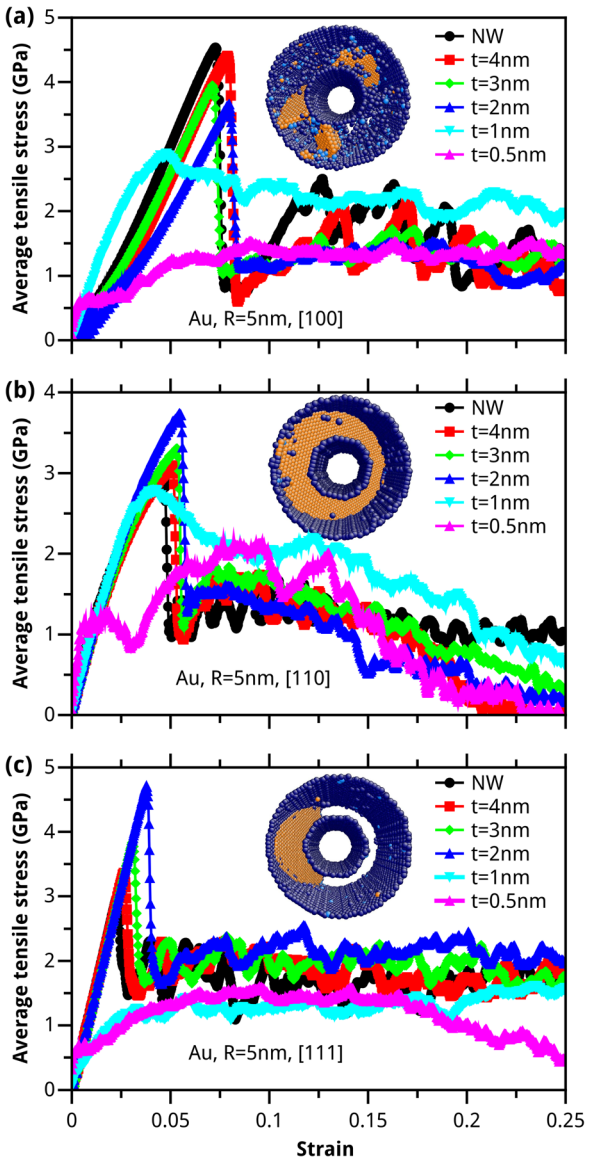

FIG. 2. Tensile stress-strain curves of Au NTs and Au NWs oriented along (a) [1 0 0], (b) [1 1 0], and (c) [1 1 1] directions of fixed outer radius $R = 5$ nm and varying wall thickness from $t = 0.5$ nm to 4 nm. The insets show the yielding modes of the respective single crystalline Au NTs. The atom colors correspond to the local lattice orientation, and the perfect fcc atoms have been removed for clarity.

solid Au NWs. For example, as compared to the defect free Au NTs ($t > 1$ nm), the yield stress in Au NTs with severe structural transformation ($t = 1$ nm and 0.5 nm) was substantially reduced as shown in Figure 2 because dislocation nucleation was relatively easy in those NWs due to the pre-formed defects. On the other hand, the plasticity in these NTs can be accommodated via the interactions between dislocations and the pre-formed structural defects, which led to significant strain hardening. The surface stress induced structural defects and morphological transformation in Au NTs with the smallest wall thicknesses thus contributed to the transition from sharp to smooth yielding that has been observed in Figure 2. It is also worth mentioning that a combination of high strength and plastic flow was enabled in [1 1 0] Au NT of $R = 5$ nm and $t = 1$ nm due to the strain-hardening effect caused by the pre-formed structural defects. Specifically, while the peak stress was comparable to that in the corresponding NW, the plastic flow stress in the [1 1 0] Au NT with $R = 5$ nm and $t = 1$ nm was consistently higher than that in the corresponding NW before the strain reached $\varepsilon = 0.2$. The high plastic flow in this particular [1 1 0] Au NT may be explained by the fact that the surface stress induced microstructural defects were mainly stacking faults and micro-twins that were parallel to the axial direction, which were relatively stable and resulted in no significant morphological transformations. Since in face-centered cubic metals the stacking faults and twin boundaries are all {111} planes, such special configuration of planar defects, e.g., parallel to the axial direction, can only be possible in [1 1 0] oriented Au NTs.

Another important trend indicated in Figure 2 was the strong size and orientation dependence of the strength and elasticity in Au NTs. Based on the stress-strain curves, the yield strength, Young's modulus, and yield strain were extracted and plotted in Figures 3(a)–3(c), respectively. Specifically, the Young's modulus in Au NTs with $t = 1$ nm and above was extracted by performing linear fits to the elastic stress-strain curves up to strain $\varepsilon = 0.02$ before significant deviation from linearity can be observed. For Au NTs with $t = 0.5$ nm, the linear fitting was applied to the initial elastic regime of the stress-strain curves up to strain $\varepsilon = 0.003$, $\varepsilon = 0.005$, and $\varepsilon = 0.00175$ for Au NTs oriented along [1 0 0], [1 1 0], and [1 1 1], respectively. On the other hand, the yield stress and yield strain in Au NTs with $t > 1$ nm which had a clear yield point and showed sharp yielding were extracted from the yield point. For Au NTs with $t = 1$ nm and $t = 0.5$ nm, the yield stress and yield strain were extracted by using the 0.2% strain offset technique. Here normalized Young's modulus E/E^* and yield strain $\varepsilon_y/\varepsilon_y^*$ were used, where the E^* and ε_y^* were the Young's modulus and yield strain in the corresponding Au NWs. A general transition in all the elastic properties can be observed when the NT wall thickness was reduced to $t = 1$ nm and below (the greyed area in Figures 3(a)–3(c)), which properly reflected the transition in stress-strain responses that has been observed in Figure 2. It was found that in Au NTs with no significant morphological transformation, e.g., when $t > 1$ nm, the change in Young's modulus as shown in Figure 3(b) due to the variation in the NT wall thickness and the resulted surface stress agreed well with previous studies by Liang *et al.*[31] In addition, the overall

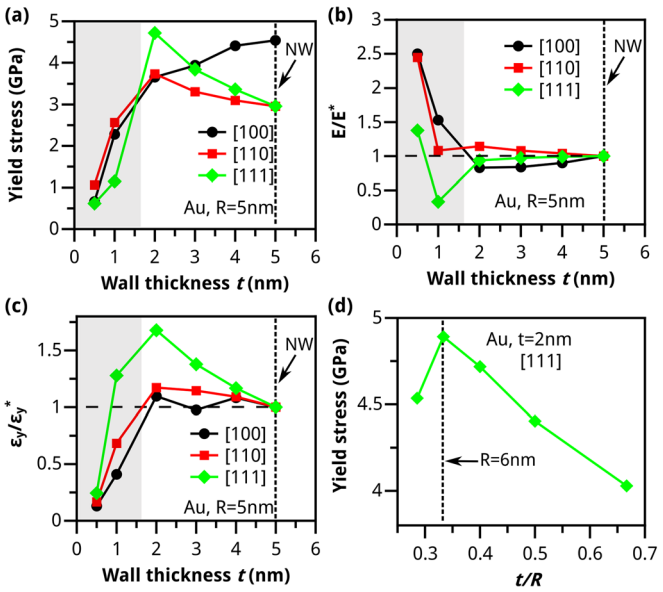

FIG. 3. (a) The yield stress, (b) normalizes Young's modulus, and (c) normalized yield strain in Au NTs oriented along [1 0 0] and [1 1 0] and [1 1 1] directions as a function of the wall thickness t. Here E^* and ε_y^* represent the Young's modulus and yield strain in the corresponding Au NWs. (d) The yield stress in [1 1 1] Au NTs of wall thickness $t = 2$ nm and outer radius varying from $R = 3$ nm to 7 nm. Dashed lines and greyed area were added as eye guide.

trend in [1 0 0] and [1 1 0] Au NWs when $t > 1$ nm agreed with Ji and Park[24] that while maintaining the outer radius, as the wall thickness decreased the yield stress and modulus decreased in [1 0 0] Au NTs but increased in [1 1 0] Au NTs. However, whilst the yield strain for both [1 0 0] and [1 1 0] Cu NTs were found to be slightly lower than the corresponding NWs by Ji and Park,[24] the opposite trend was found in this study, which might be due to the different materials, e.g., Cu vs. Au, that have been simulated.

Nevertheless, the most noteworthy results were observed in Au NTs oriented along [1 1 1] direction with $t > 1$ nm regarding both the yield strength and yield strain. While the modulus was found to be relatively unchanged (Figure 3(b)) with varying diameter,[31] the yield strain and yield stress of [1 1 1] Au NT of wall thickness $t = 2$ nm has increased by as high as 68% and 60%, respectively, as compared to the corresponding solid Au NW. Since Ji and Park[24] have suggested that the elasticity of metal NTs depended on the ratio of the NT volume to that of the corresponding solid NW, we performed another set of simulations on [1 1 1] Au NTs of fixed wall thickness ($t = 2$ nm) but varying outer radius R. The yield stress was plotted in Figure 3(d) as a function of t/R. The results were consistent with Figure 3(a) that the yield stress increased as the ratio of t/R decreased. As indicated by the vertical dashed line in Figure 3(d), the yield stress reached a maximum value with $R = 6$ nm beyond which the yield stress decreased when t/R was further decreased (or R was increased). Such observations were in line with Figure 1 that while fixing the wall thickness at $t = 2$ nm in [1 1 1] Au NTs, when R reached 7 nm and above, the surface stress became so strong that structural defects were formed in the relaxed Au NTs; those defects would dramatically lower the yield stress in Au NTs under tensile loading.

It is important to note that the yield strength reached 4.89 GPa in Au NT with $t = 2$ nm and $R = 6$ nm. Since the Schmid factor is 0.314 for yielding via nucleation of $\{1\ 1\ 1\}\langle 1\ 1\ 2\rangle$ Shockley partial dislocation (as shown in the inset of Figure 2(c)) for loading along [1 1 1] direction, the corresponding critical resolved shear stress was as high as 1.54 GPa. This value (1.54 GPa) is very close to the theoretical ideal strength for $\{1\ 1\ 1\}\langle 1\ 1\ 2\rangle$ slip in Au (1.73 GPa) as predicted by MD using the same potential for Au,[9] which is even higher than that obtained from more accurate *ab inito* calculations[32] (1.42 GPa). Therefore, instead of "adding" complex microstructures such as angstrom scale twins and surface facets,[2,9,11] here we discovered a simpler alternative approach to achieve near-ideal strength in Au NWs by "subtracting" materials from the interior.

In contrast to [1 1 0] Au NTs where the strengthening was associated with the increase in modulus, the modulus in [1 1 1] NTs was almost the same as that in the corresponding NW and the substantial strengthening must have been caused by a different mechanism. The inset of Figure 2(c) showed that the yielding of single crystalline [1 1 1] Au NTs was caused the nucleation of a Shockley partial dislocation that moved towards the inner surface. As the wall thickness decreased, the outer and inner surfaces became so close to each other that the inner surface would impose a strong repulsive image force against the nucleation of a dislocation from the outer surface. According to Deng and Sansoz,[10] the repulsive image force was reversely proportional to the distance between the two surfaces. Consequently, higher stress was needed for the yielding of Au NTs with smaller wall thickness t. The image force model may also be applied to explain the size dependent yielding in nanofilms,[33] which were similar to the metal NTs considered in this study.

While the ultrahigh strength predicted in this study may have suggested [1 1 1] metal NTs to be better candidates than corresponding solid metal NWs as building blocks in future nanotechnology, experimental validations need to be performed partially due to the extremely high strain rate used in MD simulations. For this purpose, *in situ* tensile test[2,3,34,35] that has been widely used to characterize solid metal NWs can be readily adapted for metal NTs.

In summary, we observed strong size- and orientation-dependent yielding in Au NTs through MD simulations. Particularly we revealed superelasticity and near-ideal strength in [1 1 1]-oriented Au NTs under tensile deformation. It was found that structural defects can be formed due to purely surface stress when the ratio of wall thickness to NT outer radius was reduced below certain limit, causing a transition from sharp yielding with no strain hardening to a relatively smooth yielding with strong strain hardening effects. This study offers an alternative approach of microstructural design and should stimulate further investigations on metal NTs that may have been long overlooked in the past.

This work was supported by Fudan University, China and University of Manitoba, Canada and enabled by the use of computing resources provided by WestGrid and Compute/Calcul Canada.

[1]J. R. Greer, J.-Y. Kim, and M. J. Burek, JOM J. Miner., Met. Mater. Soc. **61**, 19 (2009).
[2]J. Wang, F. Sansoz, J. Huang, Y. Liu, S. Sun, Z. Zhang, and S. X. Mao, Nat. Commun. **4**, 1742 (2013).
[3]G. Richter, K. Hillerich, D. S. Gianola, R. Monig, O. Kraft, and C. A. Volkert, Nano Lett. **9**, 3048 (2009).
[4]B. Wu, A. Heidelberg, J. J. Boland, J. E. Sader, X. Sun, and Y. Li, Nano Lett. **6**, 468 (2006).
[5]B. Wu, A. Heidelberg, and J. J. Boland, Nat. Mater. **4**, 525 (2005).
[6]A. T. Jennings and J. R. Greer, Philos. Mag. **91**, 1108 (2011).
[7]S. Hao, L. Cui, D. Jiang, X. Han, Y. Ren, J. Jiang, Y. Liu, Z. Liu, S. Mao, and Y. Wang, Science **339**, 1191 (2013).
[8]Y. F. Shao and S. Q. Wang, Scr. Mater. **62**, 419 (2010).
[9]C. Deng and F. Sansoz, ACS Nano **3**, 3001 (2009).
[10]C. Deng and F. Sansoz, Scr. Mater. **63**, 50 (2010).
[11]Y. M. Wang, F. Sansoz, T. LaGrange, R. T. Ott, J. Marian, T. W. Barbee, and A. V. Hamza, Nat. Mater. **12**, 697 (2013).
[12]B. Peng, M. Locascio, P. Zapol, S. Li, S. L. Mielke, G. C. Schatz, and H. D. Espinosa, Nat. Nanotechnol. **3**, 626 (2008).
[13]M.-F. Yu, O. Lourie, M. J. Dyer, K. Moloni, T. F. Kelly, and R. S. Ruoff, Science **287**, 637 (2000).
[14]Y. Sun, B. Mayers, and Y. Xia, Adv. Mater. **15**, 641 (2003).
[15]H. Cao, L. Wang, Y. Qiu, Q. Wu, G. Wang, L. Zhang, and X. Liu, ChemPhysChem **7**, 1500 (2006).
[16]C. Mu, Y.-X. Yu, R. M. Wang, K. Wu, D. S. Xu, and G.-L. Guo, Adv. Mater. **16**, 1550 (2004).
[17]H. Zhu, H. Chen, J. Wang, and Q. Li, Nanoscale **5**, 3742 (2013).
[18]H.-W. Wang, C.-F. Shieh, H.-Y. Chen, W.-C. Shiu, B. Russo, and G. Cao, Nanotechnology **17**, 2689 (2006).
[19]Y. Sun, B. T. Mayers, and Y. Xia, Nano Lett. **2**, 481 (2002).
[20]Y. Oshima, A. Onga, and K. Takayanagi, Phys. Rev. Lett. **91**, 205503 (2003).
[21]M. Davenport, K. Healy, and Z. S. Siwy, Nanotechnology **22**, 155301 (2011).
[22]M. J. Lagos, F. Sato, J. Bettini, V. Rodrigues, D. S. Galvão, and D. Ugarte, Nat. Nanotechnol. **4**, 149 (2009).
[23]M. V. Kamalakar and A. K. Raychaudhuri, Adv. Mater. **20**, 149 (2008).
[24]C. Ji and H. S. Park, Nanotechnology **18**, 115707 (2007).
[25]J. Diao, K. Gall, and M. L. Dunn, Nat. Mater. **2**, 656 (2003).
[26]P. A. S. Autreto, M. J. Lagos, F. Sato, J. Bettini, A. R. Rocha, V. Rodrigues, D. Ugarte, and D. S. Galvao, Phys. Rev. Lett. **106**, 065501 (2011).
[27]S. Plimpton, J. Comput. Phys. **117**, 1 (1995).
[28]G. Grochola, S. P. Russo, and I. K. Snook, J. Chem. Phys. **123**, 204719 (2005).
[29]C. Deng and F. Sansoz, Nano Lett. **9**, 1517 (2009).
[30]J. Li, Model. Simul. Mater. Sci. Eng. **11**, 173 (2003).
[31]H. Liang, M. Upmanyu, and H. Huang, Phys. Rev. B **71**, 241403 (2005).
[32]S. Ogata, J. Li, N. Hirosaki, Y. Shibutani, and S. Yip, Phys. Rev. B **70**, 104104 (2004).
[33]Y. Gan and J. K. Chen, Appl. Phys. A **95**, 357 (2009).
[34]D. S. Gianola and C. Eberl, JOM **61**, 24 (2009).
[35]Y. Zhu and H. D. Espinosa, Proc. Natl. Acad. Sci. U.S.A. **102**, 14503 (2005).